

The Photopolymerization and Cross-Linking of Electroluminescent Liquid Crystals Containing Methacrylate and Diene Photopolymerizable End Groups for Multilayer Organic Light-Emitting Diodes

Adam E. A. Contoret, Simon R. Farrar, Mary O'Neill,* and J. Edward Nicholls

Department of Physics, The University of Hull, Hull HU6 7RX, U.K.

Gary James Richards, Stephen Malcom Kelly,* and Alan William Hall

Department of Chemistry, The University of Hull, Hull HU6 7RX, U.K.

Received April 12, 2001. Revised Manuscript Received January 21, 2002

Light-emitting liquid crystals incorporating two photopolymerizable end groups have been synthesized for implementation in multilayer organic electroluminescent devices. Series of diene as well as diallylamine and methacrylate moieties are used as the photoreactive groups attached via spacers to both ends of a fluorene-based chromophore. Nematic glasses are formed upon cooling from the liquid crystalline phase. Ultraviolet radiation at room temperature is used to photopolymerize and cross-link the reactive units, resulting in the formation of insoluble nematic polymer networks. The quantum efficiency of photoluminescence from the fluorene-based chromophore is increased by cross-linking of the diene reactive end groups. Photopolymerization occurs more rapidly with methacrylate end groups, but the chromophore is somewhat degraded by the incident radiation. In materials incorporating the photopolymerizable 1,4-pentadien-3-yl group, the formation of the polymer network enhances the electroluminescence. An electron-transporting polymer containing an oxaziaoole ring is deposited on top of the insoluble network. Electroluminescence is obtained with an unchanged spectrum.

Introduction

Two distinct and successful approaches are normally used to obtain electroluminescence (EL) from organic thin films for use in organic light-emitting diodes (OLEDs). In one, uniform thin films of chromophores and charge-transporting materials of low molecular weight that form thermally stable glasses, can be deposited by thermal evaporation in vacuo.¹ Discrete thin films of different materials of low molecular weight can be sublimed in sequence using physical vapor deposition. Alternatively, cheaper and scaleable deposition methods, such as spin-casting and ink-jet printing, can be used to form electroluminescent and charge-transporting films of main-chain polymers. These thin polymer films are stabilized in the glassy state below the glass transition temperature.² The use of polymers also facilitates the production of suitable materials with high glass transition temperatures. Multilayer device structures incorporating electron-transport and hole-transport layers are often used to balance hole and electron injection and to spatially define the recombination region in OLEDs with high output efficiency. However, the deposition of multiple polymer layers

using conventional spin-coating can prove problematic, because layers can mix when solvents dissolve the underlying film. Conveniently, some hole-transporting materials such as polyethylene dioxythiophene/poly-styrene sulfonate (PEDT) are insoluble in most organic solvents and so can be covered by spin deposition of the luminescent material. However, mixing causes the application of a final electron-transporting layer to be more difficult. The most common approach to fabricating multilayer OLEDs with discrete polymer layers is the in situ thermal conversion of soluble precursor polymers, such as the alkylsulfonium precursor polyphenylene vinylene (PPV), to form insoluble polymer films.³ This approach has several disadvantages, including that wet chemistry must be performed on the device substrate and that volatile or ionic side products can be produced during the high-temperature annealing process. The latter can lead to device failure owing to damage of the polymer films or the electrodes. Here, we use a hybrid approach to obtain organic EL, combining the advantages of the ease of processing of polymers with the monodispersity of small molecules and the insolubility associated with cross-linked polymer networks. Our method should facilitate the fabrication of multilayer OLEDs and enable the realization of sub-pixelation for full-color, high-information-content dis-

(1) Chen, C. H.; Shi, J.; Tang, C. W. *Coord. Chem. Rev.* **1998**, *171*, 161.

(2) Friend, R. H.; Gymer, R. W.; Holmes, A. B.; Burroughes, J. H.; Marks, R. N.; Taliani, C.; Bradley, D. D. C.; Dos Santos, D. A.; Brédas, J. L.; Lögdlund, M.; Salaneck, W. R. *Nature* **1999**, *397*, 121.

(3) Kraft, A.; Grimsdale, A. C.; Holmes, A. B. *Angew. Chem., Int. Ed. Engl.* **1998**, *37*, 402.

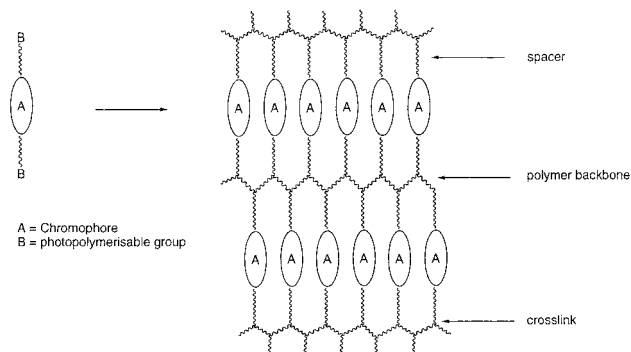


Figure 1. Illustration of the polymerization and cross-linking of a photoreactive molecule.

plays. Our hybrid approach involves the formation of thin, uniform films of electroluminescent and charge-transporting material as insoluble polymer networks. This involves the ultraviolet (UV) photopolymerization and cross-linking of mesogens with two photoreactive groups attached via aliphatic spacers to a light-emitting and/or charge-transporting chromophore. Figure 1 illustrates the general process schematically.

The use of UV exposure to render reactive polymer layers insoluble by photochemical cross-linking reactions has been reported previously. Hole-transporting side-chain polymers incorporating a cinnamate group were cross-linked by a (2+2) cycloaddition reaction, but the absorbance of the chromophore decreased during UV irradiation, indicating significant photodegradation of the chromophore.⁴ The UV-induced cross-linking of side-chain triarylamine-containing polynorbornenes was reported to create an insoluble layer, but degradation of EL performance was also observed.⁵ The cationic photopolymerization of oxetane moieties has also been used to form insoluble hole-transporting layers.^{6,7} The UV polymerization of small liquid crystalline molecules is a well-known technique for developing thermally stable passive optical devices such as retarders,^{8,9} and it has also been applied to light-emissive devices. Photoluminescence (PL)^{10–12} and EL¹³ have previously been reported from a nonemissive liquid crystalline polymer-doped network with a luminescent dye, but in the latter case, no details of the operating conditions were given. Polymerizable acrylate end groups were added to a light-emitting phenylvinylene-containing molecule, which was then aligned and thermally polymerized in the liquid crystalline state by heating to a temperature of

180 °C.¹⁴ Polarized absorbance and PL with a dichroic ratio of 3.5 were obtained. UV polymerization is preferable to thermal polymerization because it allows subpixelation by photolithographic means. However it adds another constraint on the molecular design, as a glassy or liquid crystalline phase is required at temperatures low enough to avoid thermal cross-linking. The efficacy of this approach was demonstrated using triphenylenes with bisacrylate and trisacrylate photoreactive groups. These were cross-linked by UV irradiation at temperatures above the clearing point and were used as hole-transporting layers in two-layer electroluminescent devices.¹⁵ However, the efficiency of charge transport was reduced by the cross-linking procedure.

Previously, we reported polarized EL from an aligned polymer network formed from a liquid crystalline chromophore with a diene photoreactive group.¹⁶ A polarization ratio of 11:1 was found using a photoalignment layer oriented by exposure to polarized UV radiation.¹⁷ In this paper, we compare the photopolymerization of a range of luminescent materials, each with the same chromophore but with different photoreactive groups. We show that optimal UV exposure gives insoluble polymer networks with minimal photodegradation of the chromophore. We also report EL from multilayer devices with an electron-transporting polymer deposited onto an insoluble polymer network.

Experimental Methods

Materials. The chemical structures of the photoreactive compounds 1–5 and the electron-transporting polymer 6 used in this study are shown in Table 1. The diacrylate 1, 1,4-pentadien-3-yl monomer 2, 1,6-heptadien-4-yl monomer 3, 1,4-pentadien-3-yl homologue 4, and *N,N*-diallylamine monomer 5 were synthesized from the intermediate 2,7-bis[5-(4-hydroxyphenyl)thien-2-yl]-9,9-dipropylfluorene, as shown in reaction Scheme 1. The electron-transporting polymer 6 was prepared according to a literature method.¹⁸ Fluorene, 2-(tributylstanyl)thiophene, 4-(methoxyphenyl)boronic acid, and the diene alcohols were purchased from Aldrich and used as received. Reagent-grade solvents were dried and purified as follows. *N,N*-Dimethylformamide (DMF) was dried over anhydrous P₂O₅ and purified by distillation. Butanone and methanol were distilled and stored over 5-Å molecular sieves. Triethylamine was distilled over potassium hydroxide pellets and then stored over 5-Å molecular sieves. Dichloromethane was dried by distillation over phosphorus pentoxide and then stored over 5-Å molecular sieves. Chloroform was alumina-filtered to remove any residual ethanol and then stored over 5-Å molecular sieves. ¹H nuclear magnetic resonance (NMR) spectra were obtained using a JEOL JMN-GX270 FT nuclear resonance spectrometer. Infrared (IR) spectra were recorded using a Perkin-Elmer 783 infrared spectrophotometer. Mass spectral data were obtained using a Finnegan MAT 1020 automated GC/MS. The purity of the reaction intermediates was checked using a Chrompack CP 9001 capillary gas chromatograph fitted with a 10-m CP-SIL 5CB capillary column. The purity of the final products was determined by elemental analysis.

(4) Li, X.-C.; Yong, T. M.; Gruner, J.; Holmes, A. B.; Moratti, S. C.; Cacialli, F.; Friend, R. H. *Synth. Metals* **1997**, *84*, 437.

(5) Bellmann, E.; Shaheen, S. E.; Thayumanavan, S.; Barlow, S.; Grubbs, R. H.; Marder, S. P.; Kippelen, B.; Peyghambarian, N. *Chem. Mater.* **1998**, *10*, 1668.

(6) Bayer, M. S.; Braig, T.; Nuyken, O.; Muller, D. C.; Gross, M.; Meerholz, K. *Macromol. Rapid. Commun.* **1999**, *20*, 224.

(7) Braig, T.; Muller, D. C.; Gross, M.; Meerholz, K.; Nuyken, O. *Macromol. Rapid. Commun.* **2000**, *21*, 583.

(8) Kelly, S. M. In *Flat Panel Displays, Advanced Organic Materials*; Connor, J. A., Ed.; RSC Materials Monograph; Royal Society of Chemistry: London, 2000.

(9) Van de Witte, P.; van Haaren, J.; Tuijtelars, S.; Stallinga, S.; Lub, J. *Jpn. J. Appl. Phys.* **1999**, *38*, 748.

(10) Davey, A. P.; Howard, R. G.; Blau, W. J. *J. Mater. Chem.* **1997**, *7*, 417.

(11) Sanchez, C.; Villacampa, B.; Alcalá, R.; Martínez, C.; Oriol, L.; Pinol, M. *J. Appl. Phys.* **2000**, *87*, 274.

(12) Sanchez, C.; Alcalá, R.; Cases, R.; Oriol, L.; Pinol, M. *J. Appl. Phys.* **2000**, *88*, 7124.

(13) Hikmet, R. A. M.; Braun, D. B.; Staring, A. G. J.; Schoo, H. F. M.; Lub, J. International Patent Application WO 97/07654, 1995.

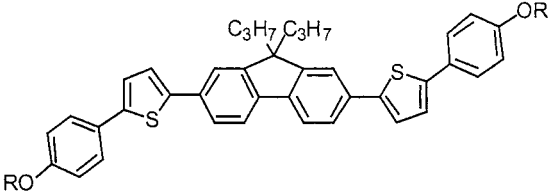
(14) Bacher, A.; Bentley, P. G.; Bradley, D. D. C.; Douglas, L. K.; Glarvey, P. A.; Grell, M.; Whitehead, K. S.; Turner, M. L. *J. Mater. Chem.* **1999**, *9*, 2985.

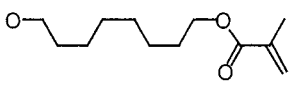
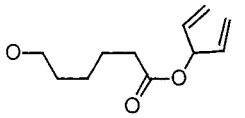
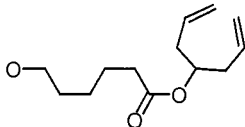
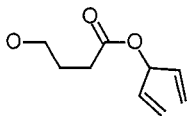
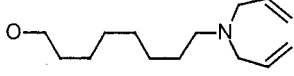
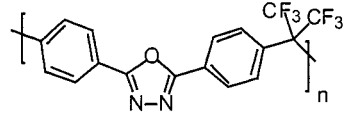
(15) Bacher, A.; Erdelen, C. H.; Paulus, W.; Ringsdorf, H.; Schmidt, H.-W.; Schuhmacher, P. *Macromolecules* **1999**, *32*, 4551.

(16) Contoret, A. E. A.; Farrar, S. R.; Jackson, P. O.; May, L.; O'Neill, M.; Nicholls, J. E.; Richards, G. J.; Kelly, S. M. *Adv. Mater.* **2000**, *12*, 971.

(17) O'Neill, M.; Kelly, S. M. *J. Phys. D: Appl. Phys.* **2000**, *33*, 67.

(18) Li, X.-C.; Kraft, A.; Cervini, R.; Spencer, G. C. W.; Cacialli, F.; Friend, R. H.; Gruner, J.; Holmes, A. B.; de Mello, J. C.; Moratti, S. C. *Mater. Res. Symp. Proc.* **1996**, *413*, 13.

Table 1. Structures and Some Transition Temperatures (°C) for the Methacrylate 1, the Dienes 2–5, and the Electron-Transporting Polymer 6^{18a}


		t_g	Cr	N	I
1	RO = 	• 10	• 69	• 120	•
2	RO = 	• 39	• 92	• 108	•
3	RO = 	• 50	• 97	(• 94)	•
4	RO = 	• 62	• 92	• 116	•
5	RO = 	• 23		• 95	•
6		•			•

^a Value in parentheses represents a monotropic transition temperature.

The liquid crystalline transition temperatures were determined using an Olympus BH-2 polarizing light microscope together with a Mettler FP52 heating stage and a Mettler FP5 temperature control unit. The thermal analysis of the photopolymerizable monomers 1–5 and the main-chain polymer 6¹⁸ was carried out with a Perkin-Elmer DSC 7 differential scanning calorimeter in conjunction with a TAC 7/3 instrument controller. Purification of intermediates and products was mainly accomplished by column chromatography using silica gel 60 (200–400 mesh) or aluminum oxide (activated, Brockman 1, ~150 mesh). Dry flash column chromatography was carried out using silica gel H (Fluka, 5–40 μ m). Electroluminescent materials were further purified by being passed through a column consisting of a layer of basic alumina, a thin layer of activated charcoal, a layer of neutral alumina and a layer of Hi-Flo filter aid using DCM as the eluent. This was followed by recrystallization from an ethanol/DCM mixture. At this stage, all glassware was thoroughly cleaned by rinsing with chromic acid followed by distilled water and then drying in an oven at 100 °C for 45 min. The purity of the final products was normally confirmed by elemental analysis using a Fisons EA 1108 CHN apparatus.

2,7-Bis(thien-2-yl)-9,9-dipropylfluorene. A mixture of 2,7-dibromo-9,9-dipropylfluorene¹⁹ (6.0 g, 0.015 mol), 2-(tributylstannyl)thiophene (13.0 g, 0.035 mol), and tetrakis(triphe-

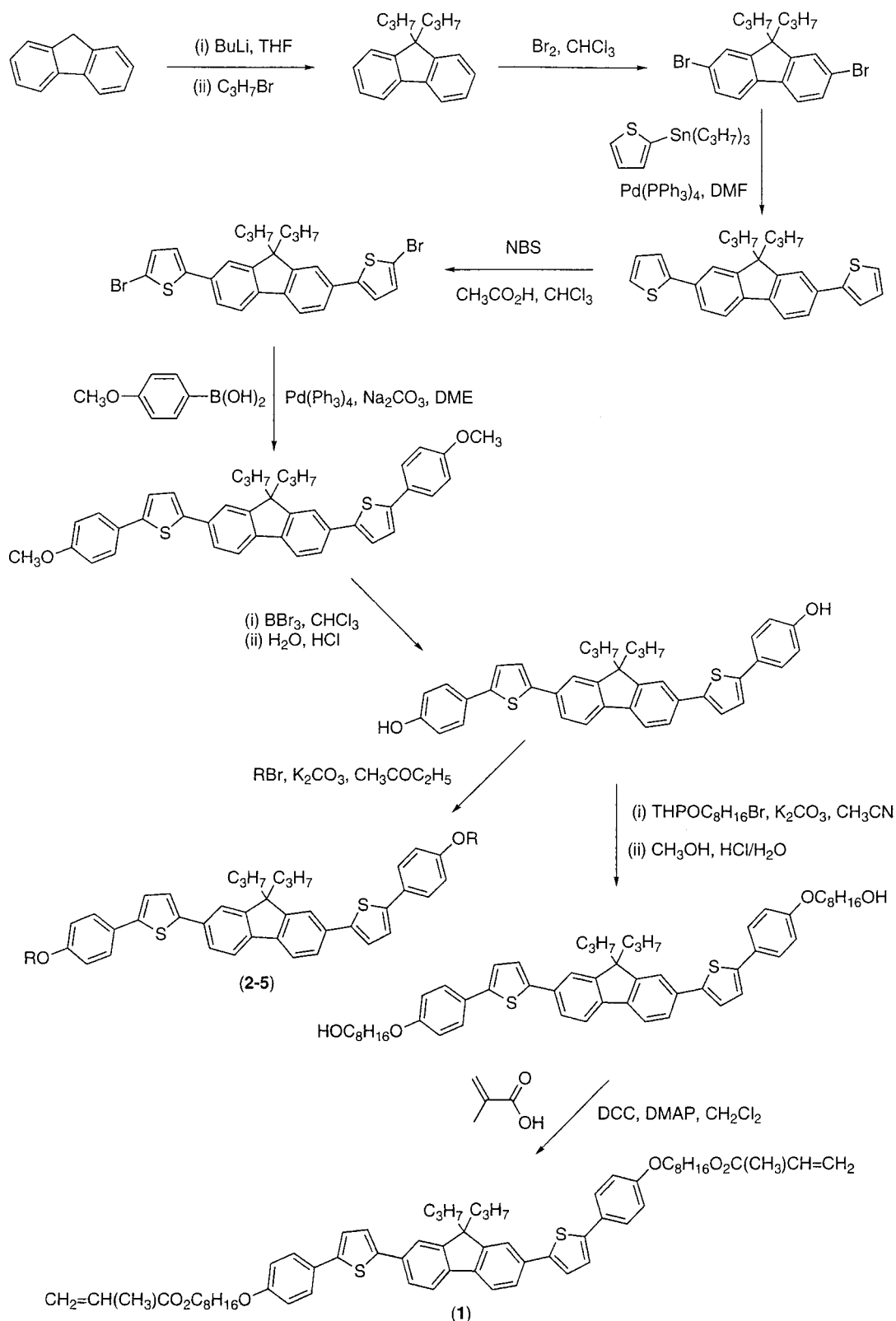
nylphosphine)palladium(0) (0.3 g, 2.6×10^{-4} mol) in DMF (30 cm³) was heated at 90 °C for 24 h. DCM (200 cm³) was added to the cooled reaction mixture, and the solution was washed with dilute hydrochloric acid (2×150 cm³, 20%) and water (100 cm³), dried (MgSO₄), and concentrated onto silica gel for purification by column chromatography (silica gel, DCM/hexane 1:1). The compound was purified by recrystallization from DCM/ethanol to yield light green crystals (4.3 g, yield 69%), mp 165–170 °C. Purity 100% (GC).

¹H NMR (CDCl₃, δ): 7.67 (2H, d), 7.60 (2H, dd), 7.57 (2H, d), 7.39 (2H, dd), 7.29 (2H, dd), 7.11 (2H, dd), 2.01 (4H, m), 0.70 (10H, m). IR (KBr pellet, cm⁻¹): 2962 (m), 2934 (m), 2872 (m), 1467 (m), 1276 (w), 1210 (m), 1052 (m), 853 (m), 817 (s), 691 (s). MS (m/z): 414 (M⁺, M100), 371, 342, 329, 297, 207, 165.

2,7-Bis(5-bromothiophen-2-yl)-9,9-dipropylfluorene. *N*-Bromosuccinimide (2.1 g, 0.012 mol, freshly purified by recrystallization from water) was added slowly to a stirred solution of 2,7-bis(thien-2-yl)-9,9-dipropylfluorene (2.3 g, 5.55×10^{-3} mol) in chloroform (25.0 cm³) and glacial acetic acid (25.0 cm³). The solution was heated under reflux for 1 h, and DCM (100 cm³) was added to the cooled reaction mixture, which was then washed with water (100 cm³), HCl (150 cm³, 20%), and saturated aqueous sodium bisulfite solution (50 cm³) and dried (MgSO₄). The solvent was removed in vacuo, and the product was purified by recrystallization from an ethanol/DCM mixture to yield yellow-green crystals (2.74 g, yield 86%), mp 160–165 °C.

(19) Kelley, C. J.; Ghiorghis A.; Kauffman, J. M. *J. Chem. Res. (M)* 1997, 2710.

Scheme 1



¹H NMR (CDCl₃, δ): 7.66 (2H, d), 7.49 (2H, dd), 7.46 (2H, d), 7.12 (2H, d), 7.05 (2H, d), 1.98 (4H, t), 0.69 (10H, m). IR (KBr pellet, cm⁻¹): 3481 (w), 2956 (s), 1468 (s), 1444 (m), 1206 (w), 1011 (w), 963 (w), 822 (m), 791 (s), 474 (w). MS (*m/z*): 572 (M⁺), 529, 500, 487, 448, 433, 420, 407, 375, 250, 126.

2,7-Bis[5-(4-Methoxyphenyl)thien-2-yl]-9,9-dipropylfluorene. A mixture of 2,7-bis(5-bromothiophen-2-yl)-9,9-dipropylfluorene (2.7 g, 4.7 × 10⁻³ mol), 4-(methoxyphenyl)boronic acid (2.15 g, 0.014 mol), tetrakis(triphenylphosphine)palladium(0)

(0.33 g, 2.9 × 10⁻⁴ mol), sodium carbonate (3.0 g, 0.029 mol), and water (20 cm³) in DME (100 cm³) was heated under reflux for 24 h. More 4-(methoxyphenyl)boronic acid (1.0 g, 6.5 × 10⁻³ mol) was added to the cooled reaction mixture, which was then heated under reflux for an additional 24 h. DMF (20 cm³) was added, the solution was heated at 110 °C for 24 h and cooled, and then dilute hydrochloric acid (100 cm³, 20%) added. The cooled reaction mixture was extracted with diethyl ether (2 × 50 cm³), and the combined ethereal extracts were washed with

water (100 cm³), dried (MgSO₄), and concentrated onto silica gel to be purified by column chromatography (silica gel, DCM/hexane 1:1) and recrystallization from an ethanol/DCM mixture to yield a green crystalline solid (1.86 g, yield 63%), Cr-N, 235 °C; N-I, 265 °C.

¹H NMR (CD₂Cl₂, δ): 7.71 (2H, dd), 7.61 (8H, m), 7.37 (2H, d), 7.24 (2H, d), 6.95 (4H, d), 3.84 (6H, s), 2.06 (4H, m), 0.71 (10H, m). IR (KBr pellet, cm⁻¹): 2961 (w), 1610 (m), 1561 (m), 1511 (s), 1474 (s), 1441 (m), 1281 (m), 1242 (s), 1170 (s), 1103 (m), 829 (m), 790 (s). MS (*m/z*): 584 (M⁺ - C₃H₇), 569, 555, 539, 525, 511, 468, 313, 277 (M100), 248, 234. Elemental analysis. Calcd (wt %): C, 78.56; H, 6.11; S, 10.23. Found (wt %): C, 78.64; H, 6.14; S, 10.25.

2,7-Bis[5-(4-hydroxyphenyl)thien-2-yl]-9,9-dipropylfluorene. A 1 M solution of boron tribromide in chloroform (9 cm³, 9.0 mmol) was added dropwise to a stirred solution of 2,7-bis[5-(4-methoxyphenyl)thien-2-yl]-9,9-dipropylfluorene (1.3 g, 2.1 × 10⁻³ mol) at 0 °C. The temperature was allowed to rise to room temperature (RT) overnight, and the solution was added to ice/water (200 cm³) with vigorous stirring. The product was extracted into diethyl ether (2 × 200 cm³), washed with aqueous sodium carbonate (2 M, 150 cm³), dried (MgSO₄), and purified by column chromatography (silica gel, DCM/diethyl ether/ethanol 40:4:1) to yield a green solid (1.2 g, yield 96%), Cr-I, 277 °C; N-I, 259 °C.

¹H NMR (d-acetone, δ): 8.56 (2H, s), 7.83 (2H, dd), 7.79 (2H, d), 7.68 (2H, dd), 7.57 (4H, dd), 7.50 (2H, dd), 7.31 (2H, dd), 6.91 (4H, dd), 2.15 (4H, m), 0.69 (10H, m). IR (KBr pellet, cm⁻¹): 3443 (s, broad), 2961 (m), 1610 (m), 1512 (m), 1474 (m), 1243 (m), 1174 (m), 1110 (w), 831 (m), 799 (s). MS (*m/z*): 598 (M⁺), 526, 419 (M100), 337.

2,7-Bis[5-[4-(8-hydroxyoctyloxy)phenyl]thien-2-yl]-9,9-dipropylfluorene. A mixture of 2,7-bis[5-(4-hydroxyphenyl)thien-2-yl]-9,9-dipropylfluorene (0.5 g, 8.4 × 10⁻⁴ mol), 2-(8-bromooctyloxy)tetrahydro-2H-pyran (0.61 g, 2.1 × 10⁻³ mol), and potassium carbonate (0.25 g, 1.8 × 10⁻³ mol) in acetonitrile (20 cm³) was heated under reflux for 24 h. Excess potassium carbonate was filtered off and rinsed with DCM (3 × 20 cm³). The solvent was removed in vacuo; methanol (50 cm³), DCM (50 cm³), and dilute hydrochloric acid (20%, 30 cm³) were added; and the solution was stirred for 2 h. The product was extracted into DCM (3 × 50 cm³), concentrated onto silica gel, and purified by column chromatography (silica gel, DCM/ethanol 40:1) followed by recrystallization from ethanol/DCM to yield the desired compound (0.4 g, yield 56%), Cr-N, 145 °C; N-I, 169 °C.

¹H NMR (CDCl₃, δ): 7.67 (2H, d), 7.60 (2H, dd), 7.57 (2H, dd), 7.57 (4H, dd), 7.33 (2H, d), 7.20 (2H, d), 6.92 (4H, d), 4.00 (4H, t), 3.66 (4H, t), 2.02 (4H, t), 1.80 (4H, quint), 1.59 (4H, quint), 1.49 (4H, quint), 1.38 (12H, m), 0.72 (10H, m). IR (KBr pellet, cm⁻¹): 3395 (m), 2939 (s), 1608 (w), 1512 (m), 1472 (s), 1286 (m), 1249 (s), 1178 (m), 1033 (m), 828 (w), 800 (m). APCI-MS (*m/z*): 855 (M⁺).

2,7-Bis[5-[4-(8-methacryloyloxyoctyloxy)phenyl]thien-2-yl]-9,9-dipropylfluorene 1. A mixture of 2,7-bis[5-[4-(8-hydroxyoctyloxy)phenyl]thien-2-yl]-9,9-dipropylfluorene (0.4 g, 4.7 × 10⁻⁴ mol), DCC (0.21 g, 1.0 × 10⁻³ mol), DMAP (0.1 g), and methacrylic acid (0.4 g, 4.7 × 10⁻³ mol) in DCM (10 cm³) was stirred for 2 days. DMF (20 cm³) was added, and the mixture was heated at 60 °C for 24 h. The solvent was removed in vacuo, DCM (20 cm³) was added, and any precipitate was filtered off. The solution was concentrated onto silica gel for purification by column chromatography (silica gel, hexane/DCM 1:1). The product was dissolved in a minimum volume of DCM and added dropwise to ethanol (50 cm³). The precipitate was filtered off and dried in vacuo (0.14 g, yield 32%), Cr-N, 69 °C; N-I, 120 °C.

¹H NMR (CDCl₃, δ): 7.67 (2H, d), 7.58 (10H, m), 7.33 (2H, d), 7.20 (2H, d), 6.92 (4H, d), 6.10 (2H, s), 5.55 (2H, s), 4.15 (4H, t), 4.00 (4H, t), 2.02 (4H, t), 1.95 (6H, s), 1.81 (4H, quint), 1.69 (4H, quint), 1.41 (14H, m), 0.70 (10H, m). IR (KBr pellet, cm⁻¹): 3418 (w), 2940 (s), 2862 (m), 1714 (s), 1607 (w), 1512 (s), 1472 (s), 1298 (m), 1249 (s), 1175 (s), 1026 (m), 829 (m), 797 (s). APCI-MS (*m/z*): 992 (M⁺). Elemental analysis. Calcd

(wt %): C, 76.33; H, 7.52; S, 6.47. Found (wt %): C, 76.29; H, 7.50; S, 6.63.

1,4-Pentadien-3-yl 6-bromohexanoate. A solution of 6-bromohexanoyl chloride (3.2 g, 0.026 mol) in DCM (30 cm³) was added dropwise to a solution of 1,4-pentadien-3-ol (2.0 g, 0.024 mol) and triethylamine (2.4 g, 0.024 mol) in DCM (30 cm³). The mixture was stirred for 1 h; washed with dilute hydrochloric acid (20%, 50 cm³), saturated potassium carbonate solution (50 cm³), and water (50 cm³); and then dried (MgSO₄) and concentrated to a brown oil. The product was purified by dry flash chromatography (silica gel, DCM) to yield a pale yellow oil (4.7 g, yield 75%). Purity >95% (GC).

¹H NMR (CDCl₃, δ): 5.82 (2H, m), 5.72 (1H, m), 5.30 (2H, d), 5.27 (2H, d), 3.42 (2H, t), 2.37 (2H, t), 1.93 (2H, m), 1.72 (2H, m), 1.54 (2H, m). IR (KBr pellet, cm⁻¹): 3095 (w), 1744 (s), 1418 (w), 1371 (w), 12521 (m), 1185 (s), 983 (m), 934 (m). MS (*m/z*): 261 (M⁺), 177, 67.

1,6-Heptadien-4-yl 5-bromopentanoate was prepared analogously to yield a pale yellow oil (1.7 g, yield 48%). Purity >92% (GC).

¹H NMR (CDCl₃, δ): 5.74 (2H, m), 5.08 (4H, m), 4.99 (1H, m), 3.41 (2H, t), 2.31 (6H, m), 1.88 (2H, m), 1.76 (2H, m). IR (film, cm⁻¹): 2952 (m), 1882 (w), 1734 (s), 1654 (m) 1563 (w), 1438 (m), 1255 (m), 1196 (s), 996 (m), 920 (s). MS (*m/z*): 275 (M⁺), 245, 219, 191, 183, 163 (M100), 135, 95, 79.

1,4-Pentadien-3-yl 4-bromobutanoate was prepared analogously to yield a pale yellow oil (1.8 g, yield 51%). Purity >85% (GC, decomposition on column).

¹H NMR (CDCl₃, δ): 5.83 (2H, m), 5.72 (1H, m), 5.27 (4H, m), 3.47 (2H, t), 2.55 (2H, t), 2.19 (2H, quint). IR (KBr pellet, cm⁻¹): 3096 (w), 2973 (w), 1740 (s), 1647 (w), 1419 (m), 1376 (m), 1198 (s), 1131 (s), 987 (s), 932 (s), 557 (w). MS (*m/z*): 217, 166, 152, 149, 125, 110, 84, 67 (M100).

2,7-Bis[5-[4-[5-(1-vinylallyloxycarbonyl)pentyl]oxy]phenyl]thien-2-yl]-9,9-dipropylfluorene 2. A mixture of 2,7-bis[5-(4-hydroxyphenyl)thien-2-yl]-9,9-dipropylfluorene (0.6 g, 1.0 × 10⁻³ mol), 1,4-pentadien-3-yl 5-bromohexanoate (0.7 g, 2.7 × 10⁻³ mol), and potassium carbonate (0.5 g, 3.6 × 10⁻³ mol) in acetonitrile (25 cm³) was heated at 50 °C for 18 h. The mixture was then heated under reflux conditions for an additional 20 h. Excess potassium carbonate was filtered off, and the precipitated product was rinsed through with DCM (2 × 30 cm³). The solution was concentrated onto silica gel for purification by column chromatography (silica gel, DCM/hexane 1:1 gradient to DCM) and recrystallization from a DCM/ethanol mixture to yield a green-yellow solid (0.4 g, yield 40%), Cr-N, 92 °C; N-I, 108 °C.

¹H NMR (CD₂Cl₂, δ): 7.69 (2H, d), 7.58 (8H, m), 7.35 (2H, d), 7.22 (2H, d), 6.91 (4H, d), 5.83 (4H, m), 5.68 (2H, m), 5.29 (2H, t), 5.25 (2H, t), 5.21 (2H, t), 5.19 (2H, t), 3.99 (4H, t), 2.37 (4H, t), 2.04 (4H, m), 1.80 (4H, quint), 1.70 (4H, quint), 1.51 (4H, quint), 0.69 (10H, m). IR (KBr pellet, cm⁻¹): 2936 (m), 2873 (m), 1738 (s), 1608 (m), 1511 (m), 1473 (s), 1282 (m), 1249 (s), 1177 (s), 1110 (m), 982 (m), 928 (m), 829 (m), 798 (s). APCI-MS (*m/z*): 958 (M⁺), 892 (M100). Elemental analysis. Calcd (wt %): C, 76.37; H, 6.93; S, 6.68. Found (wt %): C, 75.93; H, 6.95; S, 6.69.

2,7-Bis[5-[4-[5-(1-allylbut-3-enyloxycarbonyl)pentyl]oxy]phenyl]thien-2-yl]-9,9-dipropylfluorene 3 was prepared analogously to yield a green-yellow solid (0.21 g, yield 21%), Cr-I, 97 °C, N-I, 94 °C.

¹H NMR (CDCl₃, δ): 7.68 (2H, d), 7.60 (2H, dd), 7.58 (2H, d), 7.57 (2H, d), 7.33 (2H, d), 7.20 (2H, d), 6.91 (2H, d), 5.75 (4H, m), 5.08 (8H, m), 5.00 (2H, quint), 4.00 (4H, t), 2.33 (12H, m), 2.02 (4H, t), 1.82 (4H, quint), 1.71 (4H, quint), 1.53 (4H, m), 0.72 (10H, m). IR (KBr pellet, cm⁻¹): 3443 (s), 2955 (s), 1734 (s), 1643 (w), 1609 (m), 1512 (m), 1473 (s), 1249 (s), 1178 (s), 996 (m), 918 (m), 829 (m), 799 (s). APCI-MS (*m/z*): 1015 (M⁺, M100), 921. Elemental analysis. Calcd (wt %): C, 76.89; H, 7.35; S, 6.32. Found (wt %): C, 76.96; H, 7.42; S, 6.23.

2,7-Bis[5-[4-[3-(1-vinylallyloxycarbonyl)propyl]oxy]phenyl]thien-2-yl]-9,9-dipropylfluorene 4 was prepared analogously to yield a green-yellow powder (0.20 g, yield 53%), Cr-N, 92 °C; N-I, 116 °C.

¹H NMR (CDCl₃, δ): 7.61 (10H, m), 7.33 (2H, d), 7.20 (2H, d), 6.92 (4H, d), 5.85 (4H, m), 5.74 (2H, m), 5.32 (4H, d, *J* = 17 Hz), 5.24 (4H, d, *J* = 10 Hz), 4.06 (4H, t), 2.56 (4H, t), 2.16 (4H, quint), 2.05 (4H, t), 0.72 (10H, m). IR (KBr pellet, cm⁻¹): 3449 (m), 2960 (m), 1738 (s), 1609 (m), 1512 (m), 1473 (s), 1380 (w), 1249 (s), 1174 (s), 1051 (m), 936 (m), 830 (m), 799 (s). APCI-MS (*m/z*): 903 (M⁺), 837 (M100), 772. Elemental analysis. Calcd (wt %): C, 75.80; H, 6.47; S, 7.10. Found (wt %): C, 76.13; H, 6.48%; S, 6.91.

2,7-Bis[5-[4-(8-diallylaminoctyloxy)phenyl]thien-2-yl]-9,9-dipropylfluorene 5. A mixture of 2,7-bis[5-(4-hydroxyphenyl)thien-2-yl]-9,9-dipropylfluorene (0.5 g, 8.4 × 10⁻⁴ mol), toluene-4-sulfonic acid-8-diallylaminoctyl ester^{20,21} (0.8 g, 2.1 × 10⁻³ mol), and potassium carbonate (0.3 g, 2.2 × 10⁻³ mol) in butanone (30 cm³) was heated under reflux for 24 h. Excess potassium carbonate was filtered off and rinsed with DCM (3 × 30 cm³). The solution was concentrated onto silica gel for purification by column chromatography (silica gel, DCM/hexane 2:1 eluting to DCM/ethanol 4:1). The product was obtained as a yellow-green glass (0.35 g, yield 41%), N-I, 95 °C.

¹H NMR (CDCl₃, δ): 7.67 (2H, d), 7.58 (8H, m), 7.34 (2H, d), 7.20 (2H, d), 6.92 (4H, d), 5.94 (4H, m), 5.25 (8H, m), 3.99 (4H, t), 3.22 (8H, d), 2.02 (4H, t), 1.80 (4H, quint), 1.56 (4H, quint), 1.47 (4H, quint), 1.35 (12H, m), 0.71 (10H, m). IR (KBr pellet, cm⁻¹): 3437 (s), (2934 (s), 1609 (s), 1512 (s), 1472 (s), 1283 (m), 1249 (s), 1179 (s), 1031 (w), 918 (w), 829 (m), 798 (s). APCI-MS (*m/z*): 1014 (M⁺, M100), 973. Elemental analysis. Calcd (wt %): C, 79.40; H, 8.35; N, 2.76; S, 6.33. Found (wt %): C, 79.33; H, 8.29; N, 2.88; S, 6.17.

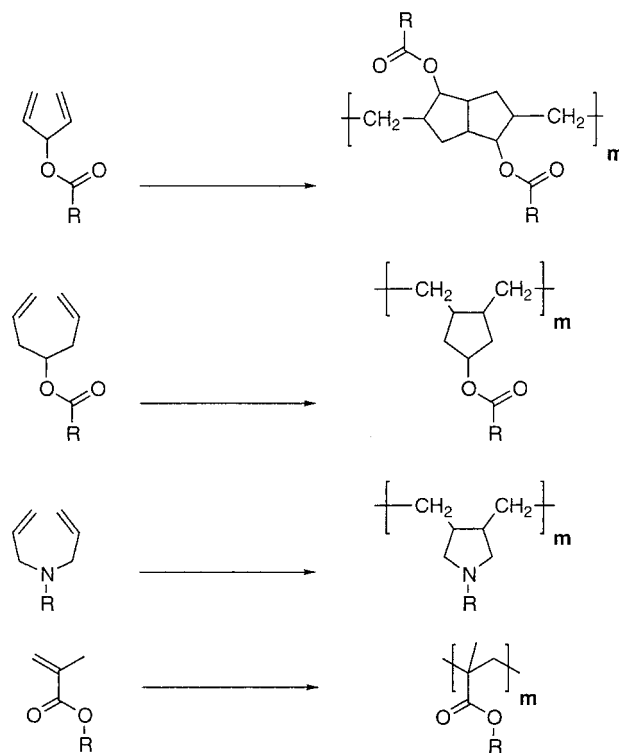
Material Processing and Evaluation. Thin films of the materials 1–5 were prepared by spin-casting from a 0.5–2 wt % solution in chloroform onto quartz substrates. All sample processing was carried out in a dry-nitrogen-filled glovebox to avoid oxygen and water contamination. The samples were subsequently baked at 50 °C for 30 min, heated to 90 °C, and then cooled at a rate of 0.2 °C to room temperature to form a nematic glass. No change in the films was observed using polarized microscopy over several months at room temperature. The films were polymerized in a nitrogen-filled chamber using light from an argon ion laser. Most of the polymerization studies were carried out at 300 nm with a constant intensity of 100 mW cm⁻²; the total fluence varied according to the exposure time. No photoinitiator was used. Temperature-dependent polymerization studies were carried out in a Linkham model LTS 350 hot stage driven by a TP 93 controller under flowing nitrogen gas. A solubility test was used to find the optimum fluence: different regions of the film were exposed to UV irradiation with different fluences, and the film was subsequently washed in chloroform for 30 s. The unpolymerized and partially polymerized regions of the film were washed away, and PL from the remaining regions was observed upon excitation with an argon ion laser at 351/362 nm. Optical absorbance measurements were made using a Unicam 5625 UV–vis spectrophotometer. PL and EL were measured with the samples mounted in a chamber filled with dry nitrogen gas using a photodiode array (Ocean Optics S2000) with a spectral range from 200 to 850 nm and a resolution of 2 nm. Films were deposited onto CaF₂ substrates for Fourier transform infrared measurements, which were carried out on a Perkin-Elmer Paragon 1000 spectrometer. Indium tin oxide- (ITO-) coated glass substrates (Merck 15Ω/□) were used for EL devices. These were cleaned using an oxygen plasma.²² A PEDT (EL-grade, Bayer) layer of thickness 45 nm (±10%) was spin-cast onto the substrate and baked at 165 °C for 30 min. This formed a hole-transporting film. One or more organic films of thickness ~45 nm were subsequently deposited by spin-casting and cross-linked as discussed below.

(20) Hall, A. W.; Lacey, D.; Buxton, P. I. *Macromol. Rapid Commun.* **1996** *17*, 417; *Macromol. Chem. Phys.* **1997**, *198*, 2307.

(21) Hall, A. W.; Goody, J. W. The University of Hull, Hull, U.K. Private communication, 2001.

(22) Kim, J. S.; Granstrom, M.; Friend, R. H.; Johansson, N.; Salaneck, W. R.; Daik, R.; Feast, W. J.; Cacialli, F. *J. Appl. Phys.* **1998**, *68*, 6859.

Scheme 2



Film thicknesses were measured using a Dektak surface profiler. Aluminum was selectively evaporated onto the films at a pressure of less than 1 × 10⁻⁵ Torr with a shadow mask to form the cathode.

Results and Discussion

Photopatternable liquid crystal networks can be formed from reactive mesogens incorporating a polymerizable end group at the end of a flexible spacer attached to each end of a molecular core (see Figure 1) and usually a radical or ionic photoinitiator. The cross-linked polymer network is formed by polymerization of each of the photoreactive end groups with nearest neighbors. A major potential problem for light-emitting materials is that the free radicals photogenerated by the photoinitiator or at the reactive group can attack the conjugated aromatic molecular core of the reactive mesogens. This is equivalent to photodegradation of the functional part of the electroluminescent or charge-transporting material, with a consequent reduction in quantum efficiency. Photodegradation is most likely to occur during the UV illumination required for cross-linking, but it can continue by accidental background exposure or electroluminescence and so reduce the lifetime of the device. We examine here the UV polymerization and cross-linking of compounds 1–5 prepared as shown in the Scheme 1. The general structures of the polymer backbones formed from the monomers are shown in Scheme 2. The methacrylate monomer 1 polymerizes by a linear radical polymerization reaction to form a relatively flexible polymethacrylate backbone. Photoreactive dienes have previously been used to form smectic side-chain polymers²⁰ and chiral nematic (cholesteric) polymer networks.²³ Cyclopolymerization of the

(23) Pfeiffer, T.; Kürschner, K.; Strohmriegel, P. *Macromol. Chem. Phys.* **1999** *200*, 2480.

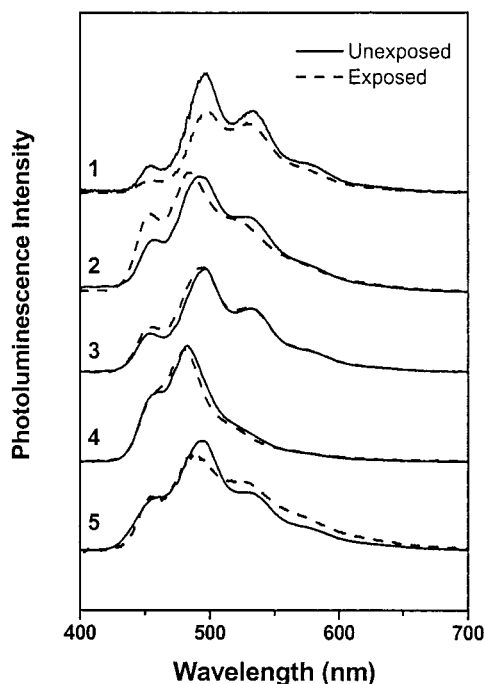


Figure 2. PL spectra from thin films of **1–5** measured before and after exposure with the optimum fluence of UV radiation to form an insoluble network. The required fluences at 300 nm are 3, 100, 100, 300, and 20 J cm⁻² for **1–5**, respectively. The films were washed after exposure.

dienes **2–5** involves a sequential intramolecular and intermolecular propagation: The ring structure is first formed by reaction of the free radical with the second double bond of the diene group.²⁴ A double ring is obtained by the cyclopolymerization of **2**, which provides a particularly rigid backbone.²⁰ The reaction is sterically controlled and is generally slower than the polymerization of the methacrylate compound **1**. Thin films of each compound were prepared and exposed to UV radiation at 300 nm. An unusual and advantageous aspect of the photopolymerization of these dienes is the absence of a photoinitiator. Solubility tests were used to find the minimum exposure required to form an insoluble network: the exposed samples were washed in chloroform for 30 s and dried before the PL spectra were measured. Figure 2 shows the PL spectra of each sample before and after illumination with the optimum fluence.

Liquid Crystalline Behavior. The liquid crystalline temperatures of the methacrylate **1** and the dienes **2–5** are collated in Table 1. All of the compounds exhibit a nematic phase with a clearing point (N–I) between 94 and 120 °C. The nematic phase of each compound was found to exhibit the typical schlieren texture with characteristic two- and four-point brushes between crossed polarizers using optical microscopy. The enthalpies of the melting and clearing points of the compounds **1–5** determined by DSC were consistent with those usually found for these transitions. The glassy state was formed on quenching each of these materials from the nematic state. The diallylamine **5** could not be obtained in the crystalline state. The melting points (Cr–N and Cr–I) of the dienes **2–4** are remarkably similar. These compounds have relatively low transition temperatures compared with those of similar molecules with six

aromatic rings in the molecular core. This probably originates from steric effects attributable to the two propyl groups in position 9 on the fluorene, as well as the branching at the ends of the aliphatic spacer groups caused by the methacrylate and diene groups. These lateral substituents increase the intermolecular distance between neighboring molecules and lower the forces of attraction between them. The high viscosity, resulting from a combination of the presence of these groups and the long aromatic molecular core, probably induces the formation of the glassy state. The methacrylate **1** exhibits the highest nematic clearing point and the lowest glass transition temperature (*t_g*) of the compounds studied. The high nematic clearing point could well result from the higher degree of branching at the ends of the terminal spacers of the dienes. This interpretation appears to be confirmed by the fact that the clearing point of the cycloheptadiene **3** is lower than that of the cyclopentadiene **2** with the same spacer length. The structure of the electron-transporting polymer **6** used to fabricate multilayer devices is also shown in Table 1.

Photopolymerization Using Diene and Acrylate End Groups. First, we examine the UV irradiation of the low-molecular-weight reactive mesogens **1** and **2** to investigate the tradeoff between polymerization of the reactive end groups at the end of the flexible spacers and photodegradation of the rigid aromatic molecular core (chromophore) for compounds with either a methacrylate or a diene photoreactive end group. The acrylate or methacrylate moieties are the most common photopolymerizable group used in liquid crystal networks, partially because of the high chemical reactivity of the radicals produced after the initiation step, i.e., the rate of the propagation step of the polymerization of the methacrylate carbon–carbon double bonds is high. However, this high chemical reactivity can also result in a correspondingly high photodegradation rate. We find that mesogens **1** and **2** require fluences of 3 and 100 J cm⁻², respectively, to form an insoluble network. Figure 2 shows the PL of compounds **1–5** before and after exposure to the optimum fluence to form an insoluble network and washing. The integrated PL intensity of methacrylate monomer **1** decreases when it is cross-linked and washed, and the PL decays similarly, but to a slightly lesser extent, without washing (see Figure 3). On the other hand, the total intensity of the PL of the diene monomer **2** increases following exposure, and the relative intensities of the vibronic peaks change. We believe that these factors are related to conformation changes imposed by the rigid cyclic polymer backbone formed from the diene monomer **2**. The additional strain imposed by the rigid backbone reduces the resonant frequency of vibration and hence the differences in energy between the PL vibronic transitions, as shown in Figure 2. Time-resolved PL experiments (to be discussed in more detail elsewhere) show that excitation transfer reduces the relative intensity of the 0–0 phonon band before cross-linking. This peak grows as a result of cross-linking, suggesting that changes in the conformation influence the spatial energy transfer rate. The methacrylate monomer **1** is significantly more photosensitive than the diene monomer **2**, requiring only 3 J cm⁻² rather than 100 J cm⁻²

(24) Butler, G. B.; Angelo, R. J. *J. Am. Chem. Soc.* **1957**, *79*, 3128.

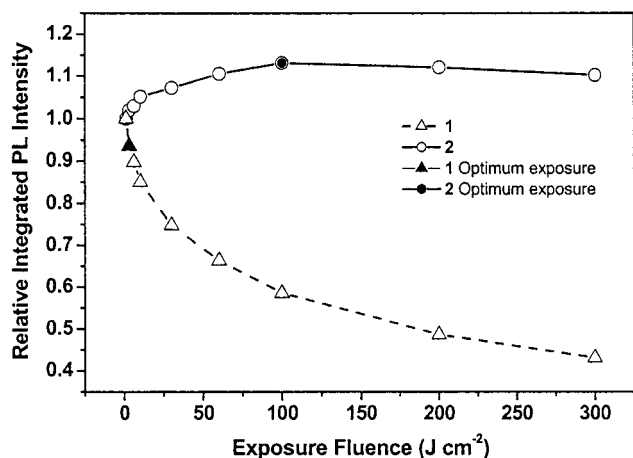


Figure 3. Integrated PL from irradiated films of **1** and **2** as a function of UV fluence. The data are normalized with respect to the PL intensity of the unexposed film.

of UV radiation to form an insoluble network. However, some photodegradation of **1** occurs even with this optimal, i.e., minimal, exposure, but some EL is still obtained from a cross-linked polymethacrylate network. Unfortunately, the high photosensitivity and chemical reactivity of **1** also result in a large tendency for continued accidental photodegradation over the lifetime of the device, owing to the high tendency of methacrylate groups to form radicals spontaneously. This is illustrated in Figure 3, which shows the integrated PL intensities from the methacrylate monomer **1** and the diene monomer **2** as a function of UV fluence up to 300 J cm⁻². These films were not washed after exposure. The integrated PL of **1** decreases sharply with fluence, whereas that of **2** remains almost constant. Hence, an electroluminescent device based on the diene monomer **2** would be more stable to subsequent accidental exposure to ambient UV radiation, as well as showing no photodegradation, when the optimum dose for cross-linking is used.

These results suggest that photodegradation of the fluorene chromophore occurs with the polymerization of methacrylate end groups, whereas little or no photodegradation is apparent when diene end groups are polymerized. A FTIR investigation was carried out to confirm that a high degree of polymerization had occurred and to examine the nature of the photodegradation. Figure 4 shows FTIR spectra of the diene monomer **2** before and after exposure with a UV light of fluence 100 J cm⁻². The difference spectrum between the two is also shown. The transitions at 932, 993, 1150, 1640, and 1737 cm⁻¹, which can be unambiguously assigned to the diene photoreactive groups, are labeled in the figure.²⁵ The difference spectrum shows a differential line shape at ~1737 cm⁻¹ corresponding to a spectral shift of the C=O transition of the diene groups as a result of cross-linking. This shift occurs because the transition is inductively coupled to the double bond, which breaks during polymerization. Further evidence for polymerization is found from the decrease in intensity of the =CH wag transitions at 993 and 932 cm⁻¹. Although not illustrated in Figure 4, an increase in

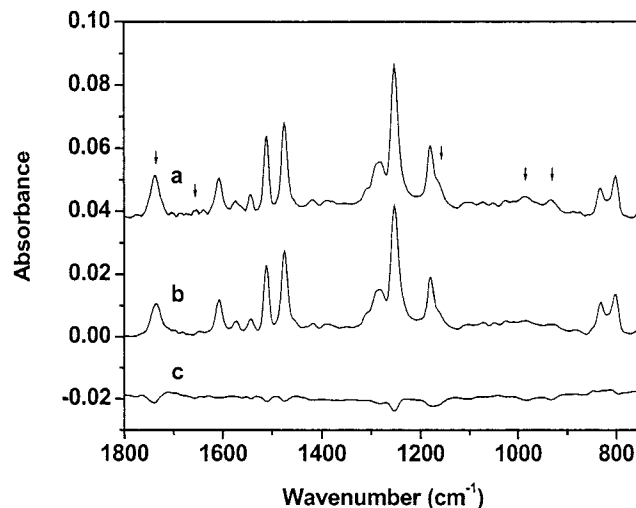


Figure 4. (a, b) IR spectrum from **2** before and after UV irradiation using a fluence of 100 J cm⁻² at 300 nm. The difference (b - a) between the IR spectra is shown in c. The arrows label the transitions originating from the diene end groups.

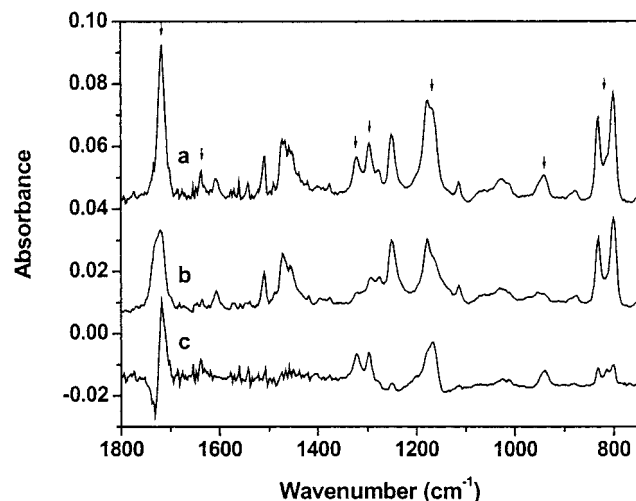


Figure 5. (a, b) IR spectrum from **1** before and after UV irradiation using a fluence of 100 J cm⁻² at 300 nm. The difference (a - b) between the IR spectra is shown in c. The arrows label the transitions originating from the methacrylate end groups.

intensity of two peaks at 2915 and 2850 cm⁻¹, originating from new aliphatic CH groups in the main-chain ring configuration, is observed after exposure. There is evidence for minor photodecomposition of the chromophore as the strength of the aromatic transitions at 1474 and 1510 cm⁻¹ decrease upon irradiation. A slightly larger decrease is shown at 1252 cm⁻¹. The latter peak originates from an alkyl phenyl ether suggesting cleavage of the flexible end chains at the ether linkage between the aliphatic spacer and the aromatic molecular core. However, both of these changes are small, <7%, and the chromophore is thus largely unaffected by UV irradiation. The FTIR and difference spectra of the methacrylate monomer **1** before and after irradiation with 100 J cm⁻² at 300 nm is shown in Figure 5. As Figure 3 shows, the PL intensity of **1** decays by 40% following this exposure. The FTIR transitions corresponding to the methacrylate group located at 815, 932, 1167, 1298, 1321, 1637, and 1718 cm⁻¹ are labeled

(25) Colthup, N. B.; Daly, L. H.; Wiberley, S. E. *Introduction to Infrared and Raman Spectroscopy*, 3rd ed.; Academic Press: New York, 1990.

in Figure 5.²⁵ The C=O transition of the methacrylate group at 1718 cm^{-1} shows a blue shift of about 15 cm^{-1} upon irradiation as a result of the breaking of the conjugated double bond. The other methacrylate transitions decrease in intensity following irradiation, thus confirming polymerization. There is also evidence for decomposition of the chromophore: in contrast to the behavior of the diene monomer **2**, the thiophene transitions at 801 and 830 cm^{-1} decrease by about 20% for the methacrylate **1** upon exposure. (The third peak observed in the difference spectrum originates from the =CH twist of the methacrylate vinyl group.) The decrease of the phenoxy transition at 1251 cm^{-1} , which indicates a cleaving of the end chains, occurs to similar extents in **1** and **2**. There is not enough evidence to prove that photodecomposition of the chromophore is responsible for all of the 40% decrease in PL intensity following irradiation. An alternative cause is the formation of nonradiative traps by free-radical reactions of the methacrylate group.

Photopolymerization Using Different Diene End Groups. We have shown above that photopolymerization can be obtained without significant photodegradation of the diene monomer **2**. We now compare the polymerization of the different diene monomers **2–5**. The optimum fluences required to polymerize the diene monomers **2–5** efficiently with a minimum of photodegradation were found to be 100, 100, 300, and 20 J cm^{-2} , respectively, using the solubility test. As Scheme 2 shows, the 1,6-heptadiene monomer **3** forms a network with a repeat unit containing a single ring. Its polymerization rate is equal to that of the 1,4-pentadiene monomer **2**, but as Figure 2 shows, **3** shows a smaller increase of PL intensity after polymerization. This might be because of the increased flexibility of the C_7 ring in the backbone of the cross-linked material. The 1,4-pentadiene diene monomers **2** and **4** are homologues and differ only in the length of the flexible alkoxy spacer part of the end groups. The PL spectrum of **4** with the shorter spacer is significantly different from those of all other materials before exposure, suggesting a different conformation. The higher fluence required to polymerize the 1,4-pentadiene monomer **4** implies that the polymerization rate is dependent on the spacer length: the freedom of motion of the photopolymerizable end group is reduced, because of the shorter aliphatic spacer in **4**. The diallylamine monomer **5** has a significantly different structure from those of the diene esters **2–4**. It is much more photosensitive than the other diene monomers because of the activation by the electron-rich nitrogen atom. Although spectral changes are observed, the PL intensity integrated over the whole spectrum is unchanged by polymerization, as shown in Figure 2. Indeed, the largest increase in PL intensity obtained by polymerization is found for the 1,4-pentadiene monomer **2**, which we chose as the best monomer for further investigation of the electroluminescent properties of this new type of polymer network formed from the photopolymerization of electroluminescent liquid crystals.

Confirmation of Optimized Photopolymerization of Monomer 2. The absorbance and PL spectra of 1,4-pentadiene monomer **2** were measured before and after exposure with the optimum UV fluence of 100 J cm^{-2} at 300 nm. The latter measurements were re-

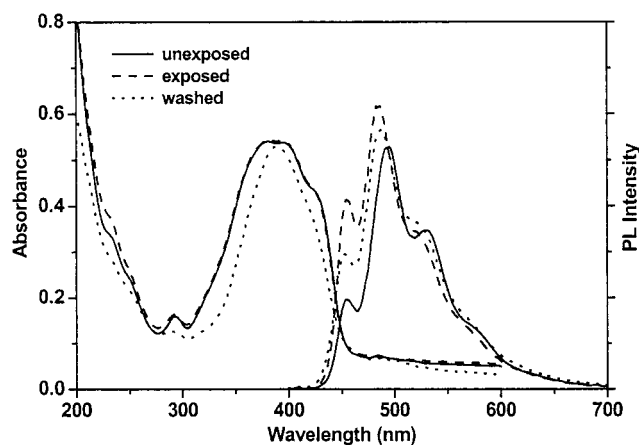


Figure 6. Absorbance and PL from **2** before and after optimal UV irradiation to form a polymer network. The spectra of the exposed films after washing are also shown.

peated after washing in chloroform for 30 s. The results are shown in Figure 6. The absorbance spectra of the unexposed and exposed films are almost identical, and the total absorbance decreases by 15% after washing, indicating that only a small amount of the material is removed. This confirms conclusively that a predominantly insoluble network is formed, as the films would be completely removed if not cross-linked.

An absolute measurement of the degree of cross-linking of reactive mesogens is usually found by monitoring the decrease in strength of the C=C FTIR transition of the photoreactive group, in combination with photodifferential scanning calorimetry.²⁶ This was impossible here because of the small oscillator strength at 1640 cm^{-1} and the presence of overlapping bands at 994 and 932 cm^{-1} . Instead, we monitored the increase in intensity of transitions from aliphatic CH groups between 3000 and 2800 cm^{-1} , resulting from the breaking of diene double bonds to form the polymer backbone. The integrated FTIR absorbance in this spectral region increases with fluence saturating at a dose above 100 J cm^{-2} .

The UV irradiation was carried out in the nematic glass phase at room temperature at 300 nm. As Figure 6 shows, excitation of the fluorene chromophore is minimal at this wavelength, and the absorbance is extremely low. The experiment was repeated using wavelengths of 351 and 362 nm near the absorbance peak. Although the number of absorbed photons is far greater at the longer wavelengths, a similar fluence is required to form an insoluble network. Furthermore, excitation at 351 and 362 nm results in some photodegradation: the integrated PL intensity decreases by 15% after application of the optimized dose. UV photopolymerization was also carried out at 300 nm at temperatures of 50, 65, and $80\text{ }^\circ\text{C}$ all in the nematic phase. It was anticipated that the polymerization rate would increase when the photoreactive mesogens were irradiated in the more mobile nematic phase. However, the fluence required to form the cross-linked network was independent of temperature, within the resolution of our solubility test. Furthermore, as Figure 7 shows, the integrated PL intensity from the cross-linked network

(26) Broer, D. J.; Boven J.; Mol, G. N. *Makromol Chem.* **1990**, *190*, 2255.

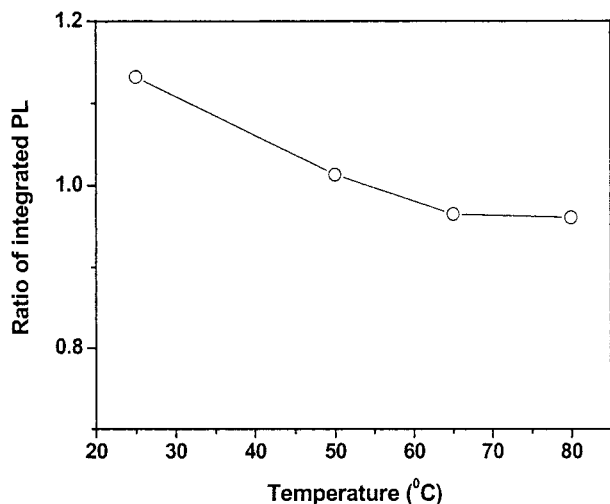


Figure 7. Ratio of the integrated PL intensity from optimally exposed and unexposed samples of **2** as a function of temperature.

decreased with temperature, indicating a temperature-dependent photodegradation.

Electroluminescent Devices. Bilayer electroluminescent devices were prepared by spin-casting the 1,4-pentadiene monomer **2** onto a hole-transporting PEDT layer. The diene **2** functioned as the light-emitting and electron-transporting material in the stable nematic glassy state. Equivalent devices using cross-linked networks formed from **2** by photopolymerization with UV were also fabricated on the same substrate under identical conditions, and the EL properties of both types of devices were evaluated and compared. The fabrication of such bilayer OLEDs is facilitated by the fact that the hole-transporting PEDT layer is insoluble in the organic solvent used to deposit the reactive mesogen **2**. Half of the layer of **2** was photopolymerized using optimum conditions, and the other half was left unexposed so that EL devices incorporating either the nematic glass or the cross-linked polymer network could be directly compared on the same substrate under identical conditions. Aluminum cathodes were deposited onto both the cross-linked and un-cross-linked regions. The integrated EL intensity from the different regions, illustrated in Figure 8, shows that EL from the cross-linked region is brighter than that from the nematic glass at the same voltage. Figure 9 shows that the threshold voltage for significant current injection is reduced by cross-linking. This suggests that the cross-linking process reduces the density of traps, assuming that the current-voltage characteristics are determined by the development of a space charge with traps. Three-layer devices were also prepared by spin-casting the electron-transporting polymer **6**, which shows a broad featureless blue emission, on top of the cross-linked nematic polymer network. Figure 10 shows the EL spectra from both the three-layer and bilayer devices operated with the same drive conditions. Identical spectra were found, showing that, in both cases, the luminescence originates from the cross-linked polymer network of the 1,4-pentadiene monomer **2**. The increased brightness of the three-layer device might result from an improved balance of electron and hole injection and/or from a shift of the recombination region away from the absorbing cathode.

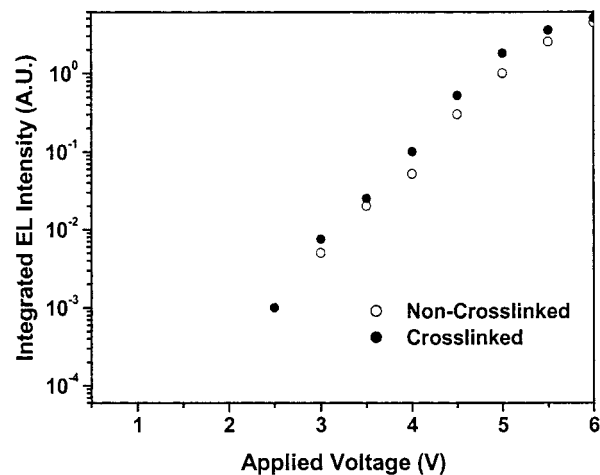


Figure 8. Voltage dependence of the integrated EL intensity from un-cross-linked and cross-linked films of **2** prepared on the same substrate.

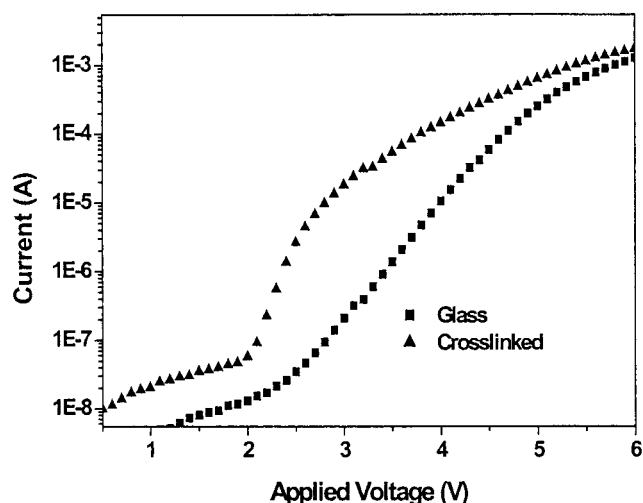


Figure 9. Current-voltage characteristics from un-cross-linked and cross-linked films of **2** prepared on the same substrate.

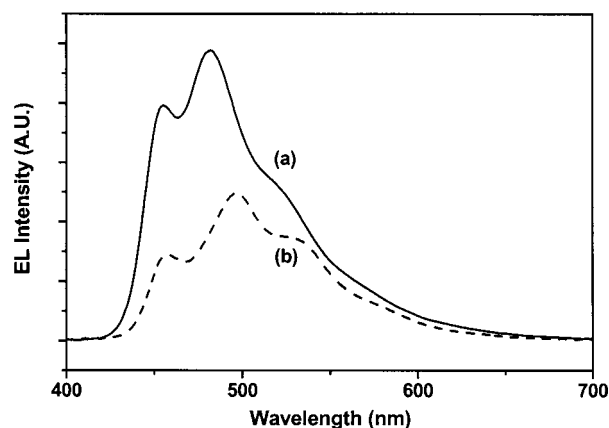


Figure 10. EL spectra from polymer network of **2** with and without an overlying layer of **6**. The same drive conditions were used for both devices.

Conclusions

We have synthesized novel light-emitting nematic liquid crystals with a range of photopolymerizable end groups, which can be polymerized and cross-linked at room temperature in the nematic glassy state (formed

on rapid cooling from the nematic phase) to create thin, insoluble cross-linked electroluminescent polymer films. Methacrylate photoreactive end groups give the fastest polymerization reaction, requiring just 3 J cm^{-2} at 300 nm but the polymerization reaction is accompanied by photodegradation of the chromophore. The polymerization of an equivalent monomer with the same chromophore, but with a 1,4-pentadiene moiety as the photopolymerizable end group instead of a methacrylate, requires 100 J cm^{-2} at 300 nm to polymerize efficiently but shows little photodegradation and an actual increase in quantum efficiency of PL from the chromophore after cross-linking. The rate of cross-linking depends on the specific structure of the diene photoreactive group. EL devices prepared using the 1,4-

pentadiene monomer **2** in the glassy state show a lower brightness at a given voltage than those prepared using the same material in the cross-linked state. The performance of these simple bilayer OLEDs can be further improved by deposition of an electron-transporting layer on top of the polymer network to form a three-layer device.

Acknowledgment. We thank the EPSRC for provision of an Advanced Fellowship (S.M.K.) and for support of this work as part of the Electronic Materials for Displays (EMD) Initiative. DERA, Malvern, U.K., is also thanked for further support.

CM011111F